Thermal Analysis of a 100 kW Polyphase Wireless Power Transfer System

Emrullah Aydin
Malatya Turgut Ozal University
Malatya, Turkey
Oak Ridge National Laboratory
Oak Ridge, USA
aydine@ornl.gov

Himel Barua
Buildings and Transportation Science Division
Oak Ridge National Laboratory
Oak Ridge, USA
baruah@ornl.gov

Ahmet Aktas
Gazi University
Ankara, Turkey
Oak Ridge National Laboratory
Oak Ridge, USA
a.aktas@gazi.edu.tr

Mostak Mohammad
Buildings and Transportation Science Division
Oak Ridge National Laboratory
Oak Ridge, USA
mohammadm@ornl.gov

Omer C. Onar
Buildings and Transportation Science Division
Oak Ridge National Laboratory
Oak Ridge, USA
onaroc@ornl.gov

Burak Ozpineci
Buildings and Transportation Science Division
Oak Ridge National Laboratory
Oak Ridge, USA
burak@ornl.gov

***Abstract*— Charging Electric Vehicles (EVs) fast and safely has a crucial role in the future of the EV technology. High-power Wireless Power Transfer (WPT) helps to significantly decrease the charging time. However, when the power transfer levels increase, thermal management becomes a significant challenge. The thermal design of the WPT systems needs more consideration in the design and implementation steps. This paper presents a thermal analysis of a 100 kW high-power WPT system. The thermal performance of the proposed design was evaluated at different power levels by considering the magnetic design and loss analysis. Finite Element Analysis (FEA) of the proposed design was performed and the thermal images of the implemented system were taken to prove the simulation results. The results show that, a liquid cooling design is needed for a high-power WPT systems for the long-time continuous operations of the charging pads.**

Keywords—thermal analysis, wireless power transfer, polyphase coil, finite element analysis

I. INTRODUCTION

Wireless charging allows systems to transfer power from source to load without a physical connection. This makes wireless charging technology a safe, convenient and reliable charging method. The long charging times and limited range of the EVs can be seen as the most important drawbacks for EV adoption, which are still standing as problems that need to be solved. To decrease the charging times, Extreme Fast Charging (XFC) has been started to be used for EV [1]. Parallel to these needs and developments in semiconductor technologies, the power levels for WPT system of EV charging have increased over the years [2-4]. The power density of a WPT system can be increased by using a three-phase system. A 50 kW system was proposed with a rotating magnetic field and a power density of 195 kW/m^2 was achieved [5].

Thermal management is one of the most critical aspects of high-power wireless charging systems. As the power level increases above 20 to 50 kW, even a highly efficient wireless charging system tends to exceed the optimal operating temperature, therefore, needs a detailed thermal analysis and design optimization. The thermal design depends on the components integrated into the charging pads. The liquid cooling becomes essential if the resonant tank components and rectifiers are added to the back of the charging pad. For a separately integrated charging pad with only coil and core, an optimally designed conductive cooling can be sufficient for a short period of charging. However, for continuous fast charging, such as 100 kW charging, liquid cooling might be required even for limiting the temperature of the coil and core.

The behavior of the charging pad parts in a WPT system changes with increasing temperature, especially with long operation durations. This causes a nonlinearity and needs to be studied carefully before an experimental verification. The thermal model of the systems can be created and analyzed by using analytical methods as given in [6]. However, developing the analytical models is a big challenge, especially for the nonlinear systems. To obtain accurate results for the thermal analysis of the WPT systems, FEA simulations can be used [7]. In the literature, the thermal design and optimization are investigated for 110 kW [8], 30 kW [9], and 50 kW [10] wireless charging systems. Other works on the thermal analysis of wireless charging systems are limited to only a few tens of kilowatt power levels [11]-[19]. However, the thermal analysis is limited for even higher-power wireless charging systems.

This manuscript has been authored by Oak Ridge National Laboratory, operated by UT-Battelle, LLC, under Contract No. DE-AC05-00OR22725 with the U.S. Department of Energy. The United States Government retains and the publisher, by accepting the article for publication, acknowledges that the United States Government retains a non-exclusive, paid-up, irrevocable, worldwide license to publish or reproduce the published form of this manuscript or allow others to do so, for United States Government purposes. The Department of Energy will provide public access to these results of federally sponsored research in accordance with the DOE Public Access Plan (http://energy.gov/downloads/doe-public-access-plan).

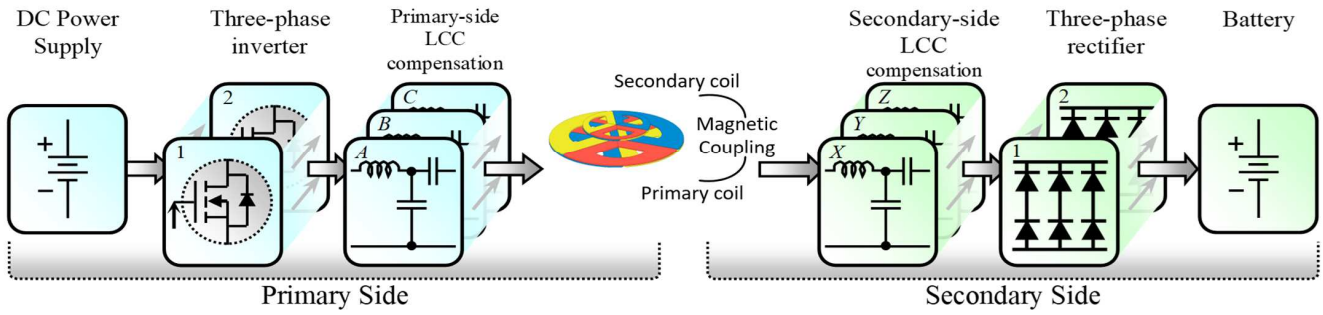

Fig. 1. Lumped structure of a three-phase WPT system.

In this paper, the thermal analysis is proposed for a highly compact, conduction-cooled 100-kW polyphase wireless charging system. In Section II, the polyphase WPT system is presented. In Section III, magnetic design and loss analysis were performed by FEA and results are given. In Section IV, thermal analysis and experimental validation of the proposed system are presented.

II. Polyphase Wireless Power Transfer System Description

A three-phase WPT system is consists of a power supply, high-frequency inverter, primary side compensation tank and primary coil. On the secondary side, there is a secondary coil, secondary side compensation tank, rectifier, and load. Polyphase coil design helps to transfer higher power levels than single-phase systems. The magnetic field for the studied three-phase WPT system is rotational and the phase coils are bipolar. A block diagram of a three-phase WPT system is given in Fig. 1.

An open-ended winding dual 3-phase inverter and an open-ended winding dual 3-phase rectifier structure were used on the primary and secondary sides respectively. According to coil inductor values on the primary and secondary sides tuning capacitors need to be added to the design to operate at the resonant frequency. Besides the basic compensation topologies, hybrid topologies can also be used to tune the system [20]. As can be seen from Fig.1, an LCC compensation topology was used for both primary and secondary sides. This topology provides a coupling coefficient and load-independent constant current [21]. As given in Fig. 1., *A*, *B*, and *C* present the primary side 3-phase coils where *X*, *Y* and *Z* present the secondary side 3-phase coils. The inductance matrix of the system is given in (1).

$$L_{3\text{-}phase} = \begin{bmatrix} L_A & M_{AB} & M_{AC} & M_{AX} & M_{AY} & M_{AZ} \\ M_{BA} & L_B & M_{BC} & M_{BX} & M_{BY} & M_{BZ} \\ M_{CA} & M_{CB} & L_C & M_{CX} & M_{CY} & M_{CZ} \\ M_{XA} & M_{XB} & M_{XC} & L_X & M_{XY} & M_{XZ} \\ M_{YA} & M_{YB} & M_{YC} & M_{YX} & L_Y & M_{YZ} \\ M_{ZA} & M_{ZB} & M_{ZC} & M_{ZX} & M_{ZY} & L_Z \end{bmatrix} \quad (1)$$

In the inductance matrix *L* indicates self-inductance and *M* indicates mutual inductance. As the power level increases, the design of the magnetic part is getting more important and the design engineers are facing some challenges. One of the most important challenges is the heating-up problems since the magnetic flux density values are increasing and they are the main reason for this.

III. Magnetic Design and Loss Analysis

The magnetic design of the WPT systems is the most important part and it consists of the coil and magnetic core materials. A 3D model of this part was created in ANSYS, Maxwell software and given in Fig. 2. FEA analysis of the model was performed to obtain the core and copper losses

The core loss for the two layers of core material and copper losses for each phase were obtained only for the secondary side since the primary side is designed quite large and a heating-up issue is not expected for this side.

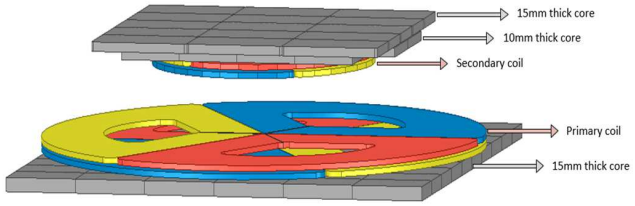

Fig. 2. Magnetic design of 100 kW WPT system.

The results show that the copper loss for the secondary side coil is 198.8 W for each phase and totally 596.4 W. The core loss for only the secondary side is 52.09 W.

The magnetic field density distribution on the secondary side core material is given in Fig. 3.

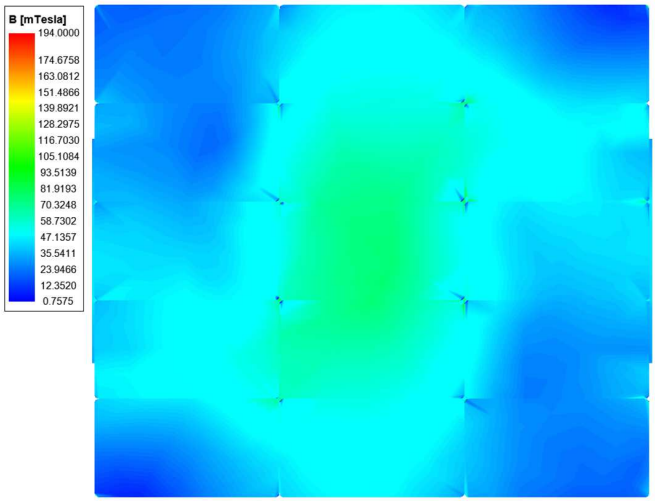

Fig. 3. FEA results of the magnetic flux density distribution over the core material.

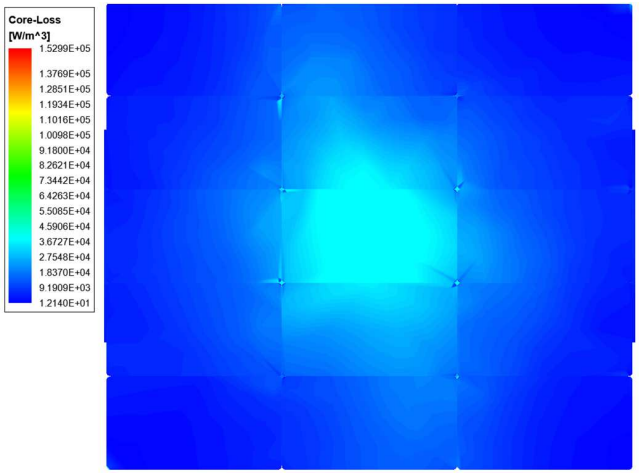

(a)

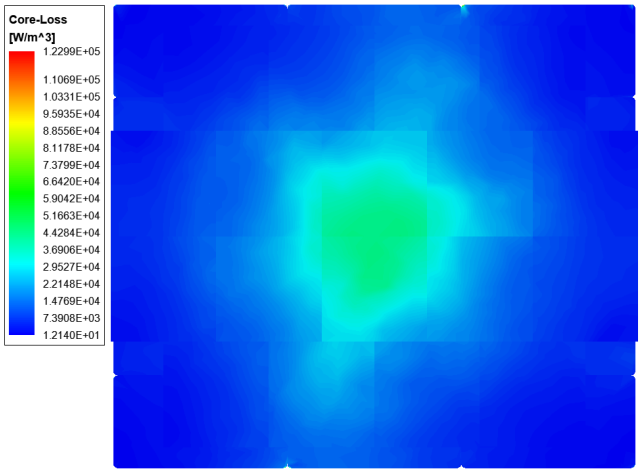

(b)

Fig. 4. FEA analysis results of the core loss distribution on the secondary side a) 15 mm thick layer top view secondary core, b) 10 mm thick layer bottom view.

The core loss distribution view on the top and bottom layers of the secondary side core material is given in Fig. 4. As can be seen from the magnetic field density and core loss distribution figures, the core loss and magnetic field concentrate in the middle since the coil design has great symmetry.

IV. Thermal Analysis and Experimental Validation

To understand the thermal behavior of the 100 kW XFC coil, transient thermal analysis was done for the secondary side of the coil. Thermal FEA was done on finite element analysis software COMSOL. Coil and core materials were the heat sources where power loss densities were assigned in the corresponding components. The losses were extracted from the electromagnetic simulation which was done one ANSYS, Maxwell. For the core losses, instead of a single finite value, the distribution of losses was assigned in the cores. In Fig. 5, the setup for the thermal analysis is given.

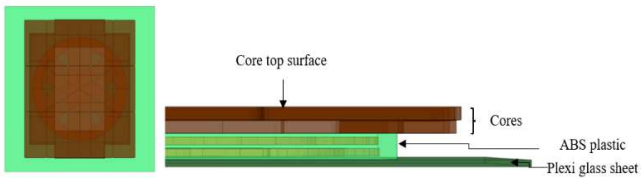

Fig. 5. Model for the thermal simulation: (a) Top view and (b) side view of the assembly.

To set the model, ABS plastic casing and plexi glass sheet were added to the model too. The plexiglass sheet is 600 mm by 600 mm and with 5 mm thickness. The ABS plastic which is used to hold the coil has similar dimensions as coil by rectangular shape. To take into account the effect of natural convective cooling, 5 W/m^2-K heat transfer coefficient was considered at all the side surfaces. At the top surface of the core which has larger exposure to air, 15 W/m^2-K heat transfer coefficient was considered to take into account the effect of higher heat transfer. At the interface of ABS plastic and the core layers, there are some holes, but due to less space from the sides, not much airflow was anticipated. So, a very conservative 1 W/m^2-K heat transfer coefficient was considered.

The thermal properties of different components are given in Table I.

TABLE I: Thermal Properties of Different Components

Components	Density (Kg/m^3)	Thermal conductivity (W/(m*K))	Temperature limit
Litz wire	4800	0.38	155
Ferrite core	4600	4.01	130
ABS plastic	1020	0.14	150
Plexiglass sheet	1150	0.13	150

After running the transient simulation for 10 minutes of WPT operation, the maximum temperature of the coil reached 90 °C while the core temperature reached to 50 °C. Fig. 6 shows the temperature of the coil with respect to time for different power losses. It shows the temperature of the coil after 10 minutes for a range of power losses starting from 10 kW to 100 kW. The initial temperature was 20 °C. For 10 kW power transfer, corresponding loss for coil is 55 W (see Table II). After 10 minutes, coil temperature reached to 26 °C. For 20 kW power transfer, where corresponding copper loss was 104.43 W, after 10 minutes, coil temperature reached to approximately 31 °C. In Table II, all the power losses in coil corresponding to relevant power transfer are provided. The core losses were extracted from the loss distribution in cores. As the distribution of losses are not uniform (see Fig. 3 and 4), core losses assigned in different position of cores are different. The center core has the highest loss density while it reduced in polynomial fashion/exponentially from the center core towards outer direction. With 10 times increment of copper loss, the coil temperature increases approximately 4 times.

TABLE II: LOSSES FOR DIFFERENT POWER TRANSFER

Power (kW)	Secondary side Copper loss per phase (W)	Secondary side Copper loss 3ph (W)	Core loss density (W/m^3)	Coil temperature (°C)
10	18.49	55.47	1.95	26
20	34.81	104.43	4.65	31
30	51.49	154.48	7.84	37
40	68.82	206.47	11.62	43
50	85.87	257.63	15.67	49
60	102.21	306.63	19.83	54
70	119.90	359.70	24.59	60
80	136.42	409.26	29.37	66
90	153.51	460.53	34.47	72
100	172.92	518.76	40.1	78

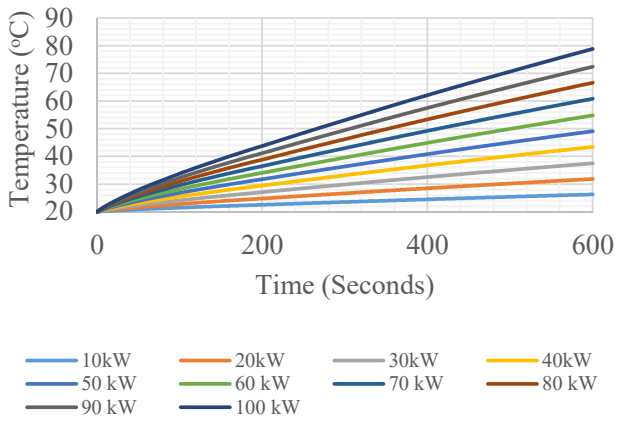

Fig. 6. Temperature change of coil with respect to time.

Fig. 7 (a) shows the contour plot to temperature in coils and Fig. 7 (b) shows the temperature distribution in core. After 10 minutes, the maximum temperature is close to the center of the coils. The core temperature distribution at the surface which is closer to the coil shows a temperature pattern similar to the coil shape.

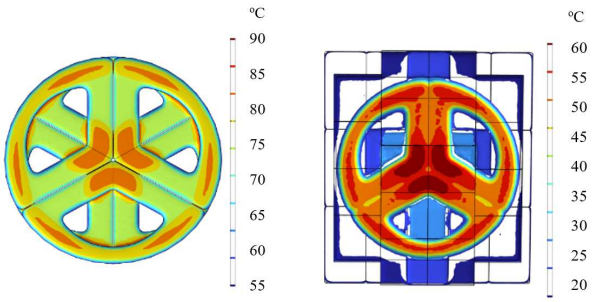

(a) (b)

Fig. 7. Temperature contour on the (a) coils and (b) core.

The surfaces which are in exposure with coil footprint, has higher temperature than surroundings. The thermal image of the experimentally implemented system was taken when the system was operating at 100 kW by FLIR Thermal Camera. The temperature distribution after 3 minutes of operation on the secondary core is given in Fig. 8.

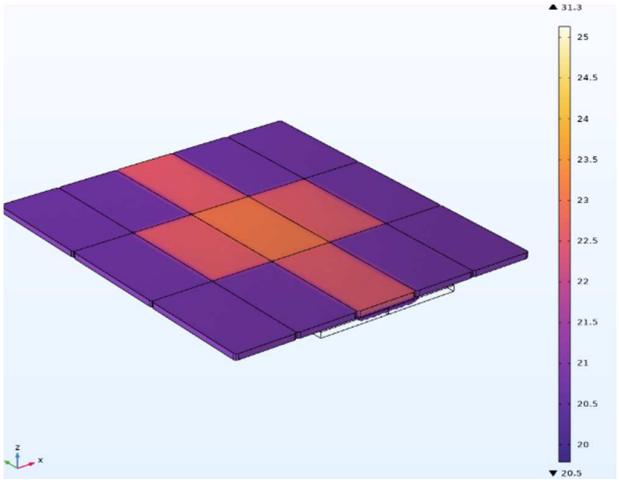

(a)

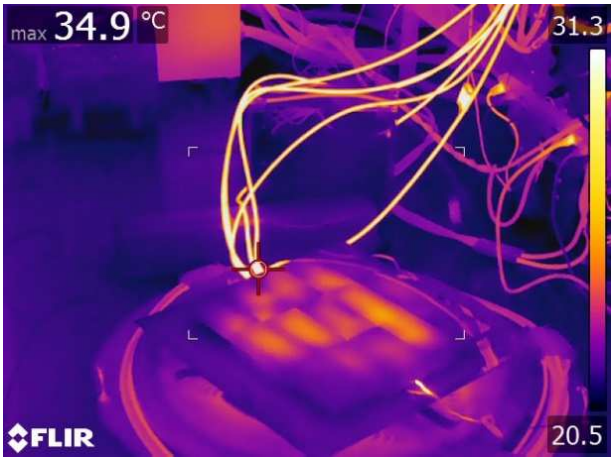

(b)

Fig. 8. Temperature distribution (°C) on the secondary core material of the 100 kW system: a) simulation result, b) experimental image.

V. CONCLUSION

In this paper, the electromagnetic loss and thermal analysis of a 100-kW polyphase wireless charging system is presented. The heat source for the thermal analysis of the wireless charging pads is the loss components of the resistive loss in the Litz wire-based coil, and hysteresis loss of the MnZn-based ferrites. The other parts affecting the thermal characteristics are the ABS coil holder, and plexiglass-based coil enclosure. The electromagnetic and thermal analysis of the studied 100 kW wireless charging system is conducted in FEA and tested experimentally at the rated power. The results show that the 100-kW charging pad can be operated with natural conduction cooling for a limited amount of time, However, for the continuous operation at rated power, it requires additional forced air or liquid cooling.

ACKNOWLEDGMENT

This research used the resources available at the Power Electronics and Electric Machinery Research Center at the National Transportation Research Center, a US Department of

Energy (DOE) Office of Energy Efficiency and Renewable Energy user facility operated by the Oak Ridge National Laboratory (ORNL). The authors would like to thank ORNL and DOE.

The authors Emrullah Aydin and Ahmet Aktas would like to thank The Scientific and Technological Research Council of Türkiye (TUBITAK) for supporting this research within the scope of the 2219 International Postdoctoral Research Fellowship Program.

REFERENCES

[1] H. Tu, H. Feng, S. Srdic and S. Lukic, "Extreme Fast Charging of Electric Vehicles: A Technology Overview," in IEEE Transactions on Transportation Electrification, vol. 5, no. 4, pp. 861-878, Dec. 2019.

[2] F. Lu, H. Zhang, H. Hofmann and C. Mi, "A high efficiency 3.3 kW loosely-coupled wireless power transfer system without magnetic material," 2015 IEEE Energy Conversion Congress and Exposition (ECCE), Montreal, QC, Canada, 2015, pp. 2282-2286.

[3] O. C. Onar, M. Chinthavali, S. L. Campbell, L. E. Seiber, C. P. White and V. P. Galigekere, "Modeling, Simulation, and Experimental Verification of a 20-kW Series-Series Wireless Power Transfer System for a Toyota RAV4 Electric Vehicle," 2018 IEEE Transportation Electrification Conference and Expo (ITEC), Long Beach, CA, USA, 2018, pp. 874-880.

[4] D. Kraus, C. Damhuis, G. Covic and H. G. Herzog, "Leakage Field and Compensation Assessment of an Interoperable High Power 50 kW Wireless Power Transfer System Using an Impedance Plane Method," 2022 Wireless Power Week (WPW), Bordeaux, France, 2022, pp. 72-77.

[5] Pries, V. P. N. Galigekere, O. C. Onar and G. -J. Su, "A 50-kW Three-Phase Wireless Power Transfer System Using Bipolar Windings and Series Resonant Networks for Rotating Magnetic Fields," in IEEE Transactions on Power Electronics, vol. 35, no. 5, pp. 4500-4517, 2020.

[6] Y. Shen, H. Wang, F. Blaabjerg, H. Zhao and T. Long, "Thermal Modeling and Design Optimization of PCB Vias and Pads," in IEEE Transactions on Power Electronics, vol. 35, no. 1, pp. 882-900, Jan. 2020.

[7] R. Wojda, V. P. Galigekere, J. Pries and O. Onar, "Thermal Analysis of Wireless Power Transfer Coils for Dynamic Wireless Electric Vehicle Charging," 2020 IEEE Transportation Electrification Conference & Expo (ITEC), Chicago, IL, USA, 2020, pp. 835-838.

[8] S. Kim et al., "Thermal Evaluation of an Inductive Power Transfer Pad for Charging Electric Vehicles," IEEE Transactions on Industrial Electronics, vol. 69, no. 1, pp. 314-322, 2022.

[9] B. Zhang et al., "Multiobjective Thermal Optimization Based on Improved Analytical Thermal Models of a 30-kW IPT System for EVs," IEEE Transactions on Transportation Electrification, vol. 9, no. 1, pp. 1910-1926, 2023.

[10] M. Mohammad, O. C. Onar, J. L. Pries, V. P. Galigekere, G.-J. Su, and J. Wilkins, "Thermal Analysis of a 50 kW Three-Phase Wireless Charging System," in 2021 IEEE Transportation Electrification Conference & Expo (ITEC), June 2021.

[11] N. Rasekh, S. Dabiri, N. Rasekh, M. Mirsalim, and M. Bahiraei, "Thermal analysis and electromagnetic characteristics of three single-sided flux pads for wireless power transfer," Journal of Cleaner Production, vol. 243, p. 118561, 2020.

[12] S. Niu, H. Yu, S. Niu, and L. Jian, "Power loss analysis and thermal assessment on wireless electric vehicle charging technology: The over-temperature risk of ground assembly needs attention," Applied Energy, vol. 275, no. 115344, Oct. 2020.

[13] S. Kim, M. Amirpour, G. Covic, and S. Bickerton, "Thermal Characterisation of a Double-D Pad," in IEEE PELS Workshop on Emerging Technologies: Wireless Power Transfer (WoW), June 2019.

[14] K. Hwang, S. Chun, U. Yoon, M. Lee, and S. Ahn, "Thermal analysis for temperature robust wireless power transfer systems," in IEEE Wireless Power Transfer (WPT), 2013.

[15] M. Alsayegh, M. Saifo, M. Clemens, and B. Schmuelling, "Magnetic and Thermal Coupled Field Analysis of Wireless Charging Systems for Electric Vehicles," IEEE Transactions on Magnetics, vol. 55, no. 6, pp. 1-4, 2019.

[16] M. Moghaddami and A. Sarwat, "Time-Dependent Multi-Physics Analysis of Inductive Power Transfer Systems," in 2018 IEEE Transportation Electrification Conference and Expo (ITEC), 2018.

[17] C. Liang et al., "Modeling and Analysis of Thermal Characteristics of Magnetic Coupler for Wireless Electric Vehicle Charging System," IEEE Access, vol. 8, pp. 173177-173185, 2020.

[18] V. Kindl, R. Pechanek, M. Zavrel, T. Kavalir, and P. Turjanica, "Inductive coupling system for electric scooter wireless charging: electromagnetic design and thermal analysis," Electrical Engineering, vol. 102, no. 1, 2020.

[19] G. R. Kalra, M. G. S. Pearce, S. Kim, D. J. Thrimawithana, and G. A. Covic, "A Power Loss Measurement Technique for Inductive Power Transfer Magnetic Couplers," IEEE Journal of Emerging and Selected Topics in Industrial Electronics, vol. 1, no. 2, pp. 113-122, 2020.

[20] Shevchenko V, Husev O, Strzelecki R, Pakhaliuk B, Poliakov N et al. Compensation Topologies in IPT Systems: Standards, Requirements, Classification, Analysis, Comparison and Application. IEEE Access 2019; vol. 7: 120559- 120580.

[21] S. Li, W. Li, J. Deng, T. D. Nguyen and C. C. Mi, "A Double-Sided LCC Compensation Network and Its Tuning Method for Wireless Power Transfer," in IEEE Transactions on Vehicular Technology, vol. 64, no. 6, pp. 2261-2273, 2015.